Simulations of directed energy thrust on rotating asteroids

Janelle Griswold[1a*], Jonathan Madajian[2a*], Isabella Johansson[a], Krysten Pfau[a], Philip Lubin[3a], Gary B. Hughes[b], Aidan Gilkes[a], Peter Meinhold[a], Caio Motta[a], Travis Brashears[a] and Qicheng Zhang[a]

[a]Physics Department, University of California, Santa Barbara, CA 93106-9530
[b]Statistics Department, California Polytechnic State University, San Luis Obispo, CA 93407-0405

ABSTRACT

Asteroids that threaten Earth could be deflected from their orbits using directed energy to vaporize the surface, as the ejected plume creates a reaction thrust that alters the asteroid's trajectory. In this situation, a critical issue is the rotation of the asteroid relative to the directed energy beam, as this will reduce the average thrust magnitude and modify the thrust direction. Flux levels required to evaporate surface material depend on the surface material composition, rotation rate, albedo, and thermal and bulk mechanical properties of the asteroid. The observed distribution of asteroid rotation rates is used, along with an estimated range of material and mechanical properties, as input to a 4D thermal-physical model to calculate the resultant thrust vector. The model uses a directed energy beam, striking the surface of a rotating sphere with specified material properties, beam profile, and rotation rate. The model calculates thermal changes in the sphere, including vaporization and mass ejection of the target material. The amount of vaporization integrated over the target is used to determine the thrust magnitude and the phase shift relative to the non-rotating case. As the object rotates beneath the beam, the energy spreads out, decreasing temperature and vaporization causing both a phase shift and magnitude decrease in the average thrust vector. This produces a 4D analytical model of the expected thrust profile for rotating objects.

Keywords: DE-STAR, Directed Energy, Laser Phased Array, Planetary Defense, Asteroid Rotation

1. INTRODUCTION

The **D**irected **E**nergy **S**ystem for **T**argeting of **A**steroids and explo**R**ation, **DE-STAR** has been proposed as a possible solution to the threat of asteroids and comets.[1] The main objective of DE-STAR is to use the focused directed energy to directly vaporize any known substance by raising its surface temperature to ~3 000 K for asteroids and 300 K for comets. This paper focus on the more difficult problem of asteroid mitigation. The process of heating the surface and the ejecting evaporated material produces a vaporization plume cloud that causes a large back-reaction force that alters the orbit of the threatening asteroid. This paper presents a method for simulating, the resultant thrust vector on asteroids from a hypothetical DE-STAR system using a 4D numeric solver (COMSOL in this case).

2. DE-STAR AND DE-STARLITE

DE-STAR is a large standoff laser phased array classified by the log of its linear size. This is discussed in a number of papers on the subject.[1,2] In order to provide full standoff protection a large array is needed to be effective with the baseline system being DE-STAR 3 or 4 (1-10 km array). Small asteroids and comets can be diverted while being vaporized with a DE-STAR 2, 100 m in length; whereas, DE-STAR 0 (1 m) and 1(10 m), can vaporize space debris. The

---

system consists of an array of phase-locked, kW class, laser power amplifiers that are driven by a common seed laser. Because the system can be phase-locked, energy can be delivered more efficiently to distant targets. The array of phase-locked modest-power laser amplifiers is powered by solar photovoltaics, of essentially the same area as the laser array. By increasing the array size, it is possible to both reduce the spot size due to diffraction and increase the power. Given a gigantic laser array, this dual effect allows the vaporization of elements on the surface of asteroids at solar-scale distances. For example, with a DE-STAR 4, vaporization could occur at over 1 AU. The flux (W/m^2) on a target scales by d^4, where d is the linear dimension of the laser array.[1]

The phased array configuration is capable of creating multiple beams; so, a single DE-STAR of sufficient size would be able to vaporize and deflect, simultaneously, multiple asteroids or one that has broken apart.[1] DE-STAR is intrinsically a multi-tasking system, the phased array configuration consists of a large number of elements that can be simultaneously used for multiple purposes and a wide variety of other functions. DE-STAR may allow standoff analysis of asteroid composition through the observation of absorption lines in the blackbody spectrum of a vaporizing surface spot.[1] As discussed in detail in Riley et al. (2014), wide-field surveys using narrow bandwidth and precision beam control would aid with asteroid identification and ephemeris refinement. The narrow bandwidth allows for extremely low background searches as well as Doppler velocity determination.[9] While DE-STAR remains a long term vision a much smaller system (DE-STARLITE) capable of being launched on a single SLS Block 1B or smaller launcher serves much the same function but requires long lead times and a dedicated mission for each target.[10] This is covered in detail in Kosmo et al. (2014). The same critical issue of rotation is relevant to both. The work presented here is applicable to both a DE-STAR and a DE-STARLITE system.

3. ASTEROIDS AND NEAR-EARTH ASTEROIDS (NEAS)

3.1. Rotation periods
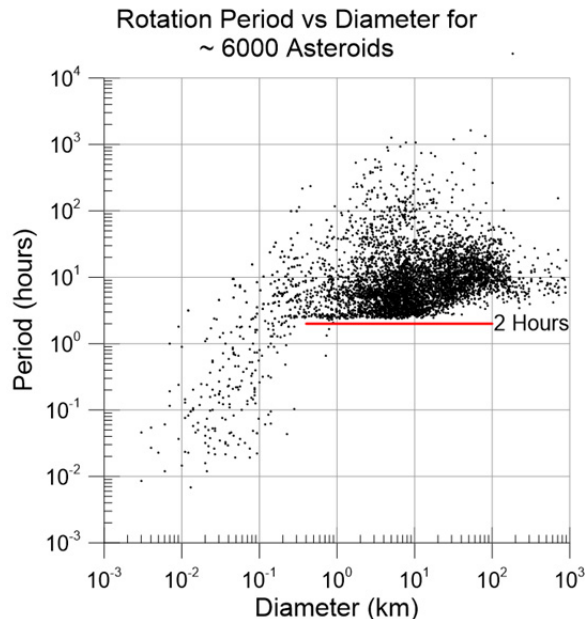
Figure 1. This graph plots the rotation periods of ~6 000 asteroids against their diameters. Notice the very sharp cutoff at just above two hours for larger diameter asteroids. Data from Minor Planet Center.[3]

Although many asteroids rotate, they are generally quite slow. A complete picture of rotation properties is not available; but, from the limited data, from the Minor Planet Center,[3] collected on the rotation of larger bodies and the break up speed. It is estimated that asteroids in the 0.1-1 km class typically rotate no faster than once per several hours; see Fig. 1.

Detailed observation of the rotation properties of more than 6 000 significantly rotating asteroids has yielded several interesting results. The asteroids in the lower left with periods less than 2.2 hours and diameters less than 0.1 km

are classified as superfast rotators and are likely molecularly bound and form a distinct population. Large asteroids (>150 m) are gravitationally bound "rubble piles" and, for these, the maximum rotation is independent of diameter and only depends on density ρ, with an angular speed ω, and rotation period τ given by:

$$\omega = \sqrt{\frac{4}{3}G\rho} = \frac{2\pi}{\tau} \Rightarrow \tau = \sqrt{\frac{3\pi}{G\rho}}$$
(3.1.1)

$$\tau \approx 1.19 \times 10^4 \rho [g/cm^3]^{-1/2} s \approx 3.3 \rho^{-1/2} [hr]$$
(3.1.2)

Notice that both angular speed and rotation period are dependent on density and independent of diameter. Estimated densities are in the range of $\rho \sim 2$ g/cm^3 yielding a minimum rotation period of about 2.3 hours. This is evident in Fig. 1.

The cutoff in rotation periods is observed to be remarkably sharp (see Fig. 1), and lies very close to 2 hours for asteroids of diameters greater than approximately 150 m, consistent with equation 3.1.1. Some smaller asteroids rotate faster, as they can be molecularly bounds instead of simply gravitationally bound (such as an iron meteorite), but these are relatively rare in large diameters.

Even fast rotating asteroids can be mitigated, since the mass ejection begins so quickly after the laser is turned on. As is seen in the transient thermal simulations below, the mass ejection (and hence thrust) begin within about 1 second for virtually all materials and all sizes of DE-STAR and DE-STARLITE. Since flux is the critical variable, the same flux at any distance will induce the same mass ejection flux for the same asteroid composition. In general, asteroids are quite dark at a baseline wavelength (1 μm), with typical reflectivity of 5-10%. This paper will discuss the time scale to spin down and stop rotating asteroids of varying sizes and initial rotation rates vs different sized DESTAR systems. The same system can be used to spin up an asteroid, possibly to the gravitational disruption limit.

3.2. The Yarkovsky-O'Keefe-Radzievskii-Paddack (YORP) Effect

The spin rate of asteroids can either increase or decrease by means of a propulsion effect due to thermal re-emission of photons from the sun onto the surface of an asteroid known as the Yarkovsky-O'Keefe-Radzievskii-Paddack (YORP) effect, a non-gravitational effect. The overall propulsion force causes a net torque, which ultimately can change the period, axis of rotation, and direction of rotation. Although the force applied onto the asteroid is quite small, this can result in a very large rotation rate change. Asteroids with spin axes perpendicular to their orbital plane, also called prograde rotators, are driven in the direction of orbit, additionally, due to the YORP effect, their spin rates are increased[11]. Furthermore, asteroids with a retrograde rotation are pushed backwards, slowing down their spin. The asteroid 1862 Apollo (diameter of 1 400 km) has been observed to increase in one additional orbit rotation cycle over the last 40 years, resulting in a decrease in its orbit rotation period. Because of the changes of the spin rate and orbit rotation period, some speculate that the YORP effect causes structural alterations on the surface due to mass shedding, thus reducing angular momentum.[7] In the process of predicting changes in momentum, many factors must be taken into consideration such as size, shape, spin, and mass.

Observed changes in spinning rates are in reasonable agreement with theoretical calculations, and the YORP effect explains the anomalous distribution of spin rates of asteroids under 10 km in diameter. Another factor that influences the YORP effect is the thermal conductivity of compounds on the asteroid's surface. If the spin rate and shape are known, the YORP effect could be used to model accurate trajectories. Through observation of the strength of the YORP effect, it is also possible to estimate the mass of small asteroids; additionally, given that the shape and size are known sufficiently well, density could also be inferred.

3.3. Thermo-Mechanical Properties of Asteroids

Unfortunately, it is not possible to bring asteroids into the laboratory to study their thermal properties, so it is necessary to rely on astronomical observations, primarily in the infrared, combined with assumptions about their formation and likely structure, to deduce their properties. Several references[3,4,5,6], among many others, have conducted excellent work in this area and it is possible to use results presented in those papers to derive the thermal properties by studying the time varying temperature as deduced from infrared observations. In this way, the thermal inertia Γ (J/m^2 K s$^{1/2}$) and thermal conductivity K [W/m K] are derived. The relationship between the terms is:

$$\Gamma = [\rho \cdot K \cdot C]^{1/2}$$
(3.3.1)

$$K = \frac{\Gamma^2}{\rho \cdot C} \tag{3.3.2}$$

Where:

Γ = thermal inertia (J/m^2 K s$^{1/2}$)

K = thermal conductivity [W/m K]

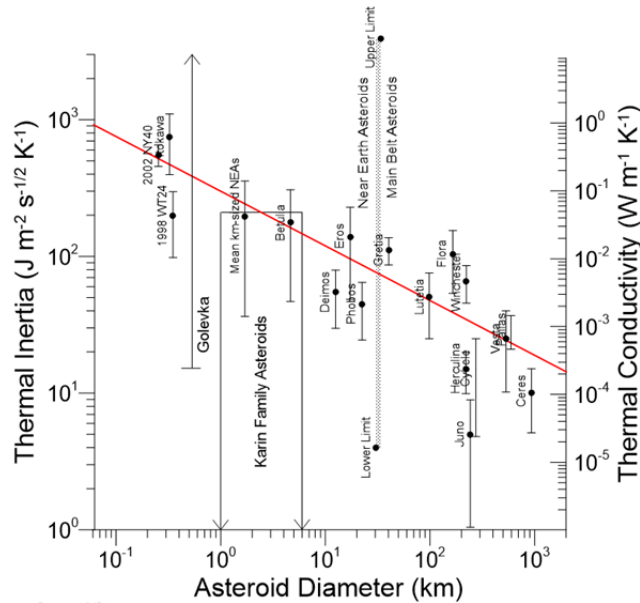ρ = density [kg/m^3]

C = heat capacity [J/kg K]

The curve shown in Fig. 2 represents best fit to data[6], where D is the asteroid diameter [km] is:

$$\Gamma = d \cdot D^{-\zeta} \tag{3.3.3}$$

With d = 300 [km], ξ = 0.4:

$$K = \frac{9 \cdot 10^4 \cdot D^{-0.8}}{\rho \cdot C} \tag{3.3.4}$$

Figure 2. Thermal Inertia Γ [J/m^2 K s$^{1/2}$] and Thermal Conductivity: K [W/m K]

The trend (*with some significant deviations*) is towards smaller asteroids having larger thermal conductivity and larger asteroids having smaller thermal conductivity. Some of this may be the point contacts from "rock pile" effect for larger asteroids. A similar trend between asteroid size and thermal inertia is also observed. It is the thermal conductivity that is important in the thermal simulations though, below K~ 10 W/m K there is little effect on the mass ejection rates and thus on the thrust. A relatively conservative case of K = 1 [W/m K] is assumed for the majority of models presented. To put this in perspective, some values for common materials are given in Table 1.

Increased thermal conductivity results in lower final spot temperatures of the asteroid target as shown in Fig. 3. For example in a small DE_STARLITE case of raising the laser power from 10 kW to 20 kW resulted in slightly smaller range between minimum (cold portion of the asteroid) and maximum (center of the laser spot) final (spot) temperatures, and yet revealed a relatively small effect on the final temperature between the two laser powers. For this case, K= 1 W/m K was used. Models were ran where the thermal conductivity varied between 0.01 and 250 W/m K; even here, the evaporation mass flux and thrust change only slightly, shown in Fig. 3.

Material	K [W/m K]	ρ [kg/m^3]	C [J/kg K]	Γ [J/m^2 K s$^{1/2}$]
Nickel	91	8850	448	1.9x10^4
Iron	81	7860	452	1.7x10^4
Granite	2.9	2750	890	2600
Ice (solid)	2.3	917	2000	2040
SiO$_2$ (solid)	**1.04 (*at 200 °C*)**	**2200**	**1000**	**1510**
Water (liq 0°C)	0.56	1000	4200	1500
Snow (firm)	0.46	560	2100	740
Soil (sandy)	0.27	1650	800	600
Pumice	0.15	800	900 (*varies significantly*)	330
Styrofoam	0.03	50	1500	47
Air	0.026	1.2	1000	5.6
Moon (regolith)	0.0029	1400	640	51

Table 1. Common material thermal properties for comparison to the asteroid thermal properties in Fig. 2

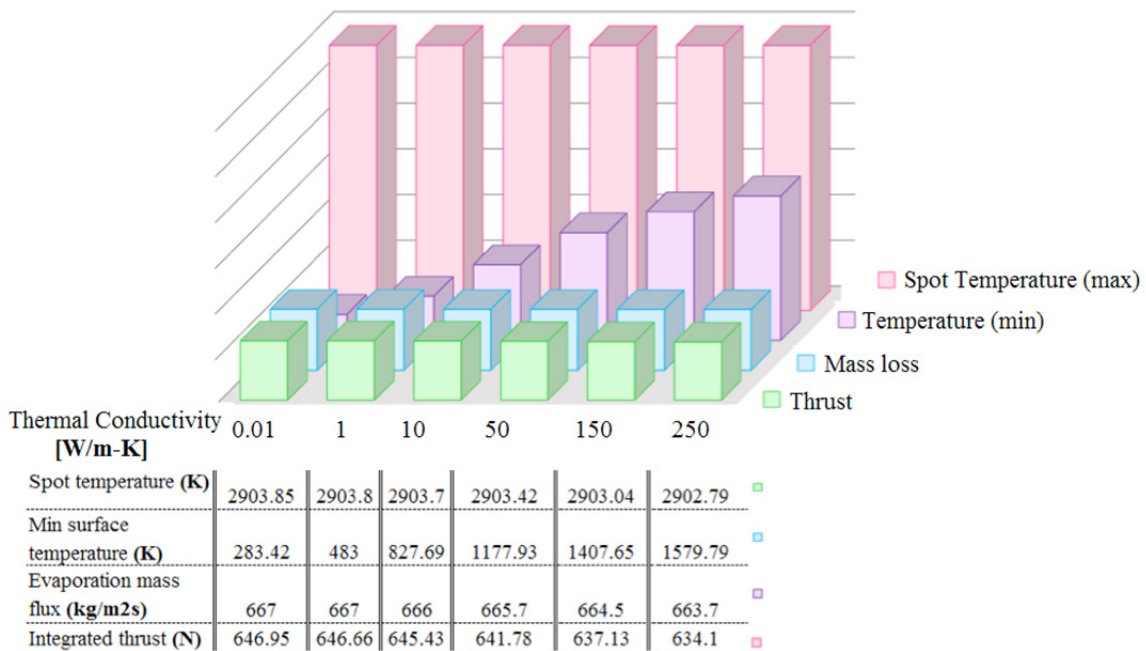| Thermal Conductivity [W/m-K]	0.01	1	10	50	150	250	
Spot temperature (K)	2903.85	2903.8	2903.7	2903.42	2903.04	2902.79	
Min surface temperature (K)	283.42	483	827.69	1177.93	1407.65	1579.79	
Evaporation mass flux (kg/m2s)	667	667	666	665.7	664.5	663.7	
Integrated thrust (N)	646.95	646.66	645.43	641.78	637.13	634.1	

Figure 3. Extreme values inputs of thermal conductivity set to 0.01-250 W/m K for SiO$_2$ – Using 1 MW laser power, spot diameter is 60 mm, with sigma of beam width of 10 mm, in this case for a 2 m diameter asteroid.

4. THERMAL ANALYSIS MODELS IN COMSOL

4.1. Thermal conduction Flux levels required for vaporization and thrust plume

Radiation goes as the 4th power of T, while the mass ejection from evaporation goes roughly exponentially in T. At low flux levels, the outward flow is completely dominated by radiation (the asteroid is heated slightly and it radiates). As the spot flux level increases (spot size shrinks or power increases or both), evaporation becomes increasingly dominant and, eventually, at about T ~ 2 000 - 3 000 K or fluxes of 10^6 - 10^7 W/m^2, mass ejection by evaporation becomes the dominant outward power flow. Just like water boiling on a stove, as flux increases, the temperature stabilizes and only the rate of mass ejection increases.[1]

In the mass ejection model, where Γ_e is the mass ejection flux [kg/m^2 s], and H$_v$ is the heat of vaporization [J/kg]. The heat of fusion, H$_f$, is included for relevant cases. The heat of sublimation is the sum of the heat of

vaporization and heat of fusion. H_f is typically a small fraction of H_v. The mass ejection flux Γ_e can be approximated by calculating the vapor pressure as follows:

$$\Gamma_e = \frac{M\alpha_e(P_v - P_h)}{\sqrt{2\pi MRT}} = M^{1/2}(2\pi RT)^{-1/2}\alpha_e(P_v - P_h) \tag{4.1.1}$$

Where:

$M\ =\ $ Molar mass $[\text{kg}/\text{mol}]$
$P_v =\ $ Vapor pressure $[\text{Pa}]$
$P_h =\ $ Ambient vapor pressure $[\text{Pa}]$ $(P_h\ =\ 0\ \text{in vacuum})$
$\alpha_e = \text{coef. of evaporation }(0 \leq \alpha_e \leq 1) - \text{ typically empirically determined}$

The models vapor pressure for each element and compound is determined using a semi analytic form known as Antoine coefficients A, B, and C in the following equation:

$$\log(P_v) = A - \frac{B}{T+C} \tag{4.1.2}$$

Where A, B and C are unique per element and compound. Hence:

$$P_v = 10^{A - \frac{B}{T+C}} \tag{4.1.3}$$

And

$$|\vec{F}_{\text{Ejecta}}| = M^{1/2}\frac{1}{\sqrt{2\pi RT}}\alpha_e 10^{A - \frac{B}{T+C}} H_V \tag{4.1.4}$$

Although it is not critical, the laser spot is approximated with a Gaussian profile, where the Gaussian laser power is P_T, is the laser flux is F_L [W/m^2], the distance from the spot cent is r [m], and the standard deviation of the Gaussian beam is sigma.

$$|\vec{F_L}| = \frac{P_T}{2\pi\sigma^2}e^{\frac{-r^2}{2\sigma^2}} \tag{4.1.5}$$

In the approximation where the spot is small compared to the asteroid, the equation becomes:

$$\vec{F_L} = \frac{-P_T}{2\pi\sigma^2}e^{\frac{-r^2}{2\sigma^2}}\hat{n} \tag{4.1.6}$$

The Gaussian approximation to the laser profile also provides temperature, vapor pressure, and mass ejection flux– T, P_v, and Γ_e as functions of the distance from the center of the laser spot. Defining these parameters allows us to determine the time per sigma, which is the amount of dwell time, spent in one Gaussian beam sigma or the amount of time it takes for the laser to cover a distance of one sigma. Time per sigma is a critical and predictive value; values greater than roughly 1 second allow strong mass ejection to occur.

4.2. Previous models and 3D Thermal-Physical Model

The thrust produced by DE-STAR on an asteroid was previously calculated using three different modeling approaches, each increasing in complexity and realism.[2] The first method used was a 1D Energetics model. In this method, only vaporization was included. By, assuming the system is completely radiation dominated, asteroids are heated to their radiation point of about 2 000 – 3 000 K using the heat of vaporization along with a set spot flux that corresponded to a temperature of approximately 6 000 K. This lead us to compute the evaporation flux or the mass ejection rate, $M_e = P_T/H_v$, where P_T is the laser power needed to heat the spot above the radiation point.

A 2D Analytic method is then used, which modeled vapor pressure versus temperature, including radiation emission while ignoring thermal conduction. It is assumed that thermal conduction is small compared to radiation and mass ejection. To show the effects of non-ideal beam formation as well as beam and pointing jitter, the parameter sigma (σ) in the Gaussian beam was varied. For a DE-STAR 4 at 1 AU, σ is diffraction-limited to about 5 m. It was found that,

as long as the power is high enough, then the system was extremely tolerant to errors in beam formation, focus, beam jitter, and pointing errors beyond 10σ. For the small DE-STARLITE mission, the situation is similar but the spot is much smaller, typically on the order of 1 cm.

The final method was a 3D and 4D (dynamics) numeric Fine Element Analysis, (FEA), model that included phase change, vapor pressure, mass ejection, radiation, and thermal conductivity. Time evolution was added to the 3D solver to understand the mass ejection over time under dynamic situations. Fig. 4 shows the temperature of the center of the spot on a time evolution model compared to a stationary model. Both models yield equal surface temperature distribution and rise to the point of being mass ejection limited, which is approximately 2 600 K in the center of the spot.[2] In this example the laser beam is rotated around the asteroid to clearly show the cooling of the spot as the target rotates. Results from the three analyses were previously reported, and all three models yielded consistent answers.[2]
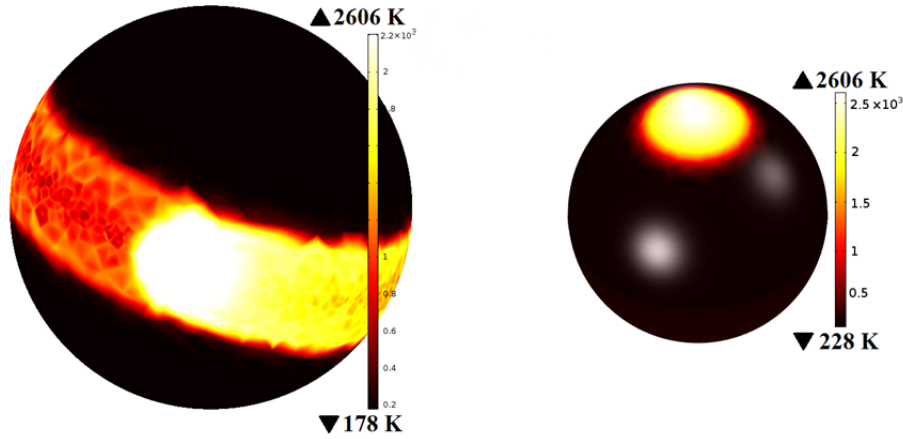
Figure 4. Rotating and stationary 3D plots for SiO_2: Using 1 hour rotation period for a 100 m diameter asteroid with a large DE-STAR 4 case of 50 GW laser power at 1 AU, yields equal surface temperature distribution as in the stationary steady state case. A very similar image occurs with a small 100 kW DE-STARLITE mission with a small spot (~ 1cm) for a dedicated standoff mission.

4.3. 4D Analytical Model

As the object rotates beneath the directed energy beam and the temperature drops, vaporization decreases, causing both a phase shift and magnitude decrease in the average thrust vector. From the Antoine Coefficients (A, B, and C) and the previous 3D model's temperature solutions, it is possible to calculate the vapor pressure, P_v, [Pa]. Note the Antoine coefficients A,B,C are often given for pressure in mm Hg and T is in Celsius. The conversion to pressure in Pa and temperature T in Kelvin is shown below:

$$P_V = (Pa) = 133.32 \times 10^{\left(A - \frac{B}{C+T-273.15}\right)} \tag{4.3.1}$$

The following surface integrals were then calculated to determine the thrust vector, at each point in time, producing a 4D analytical model of the expected thrust profile for rotating objects.

$$\overrightarrow{F_T} = \left\{ -\iint \frac{P_V x}{R}, \quad -\iint \frac{P_V y}{R}, \quad -\iint \frac{P_V z}{R} \right\} \tag{4.3.2}$$

This next example is for a DE-STARLITE case with a 1 MW laser. Although this is a larger DE-STARLITE mission, it still fits in a single launcher. A normalized thrust vector showed that, as the time per sigma (with units of seconds) increased, both the thrust [N] and the thrust per watts [N/W] increased rapidly until approximately 1 second. Then, the thrust increases as the time per sigma increases (slower asteroid), beginning to level out to its maximum, shown in Fig. 5. Fig. 6 shows the same trend, but with a max thrust per watt of ~ 5.3×10^{-4} N/W for time per sigma greater than about 10 seconds. Figure 7 shows another DE-STARLITE case that follows a similar trend as the 1 MW case.
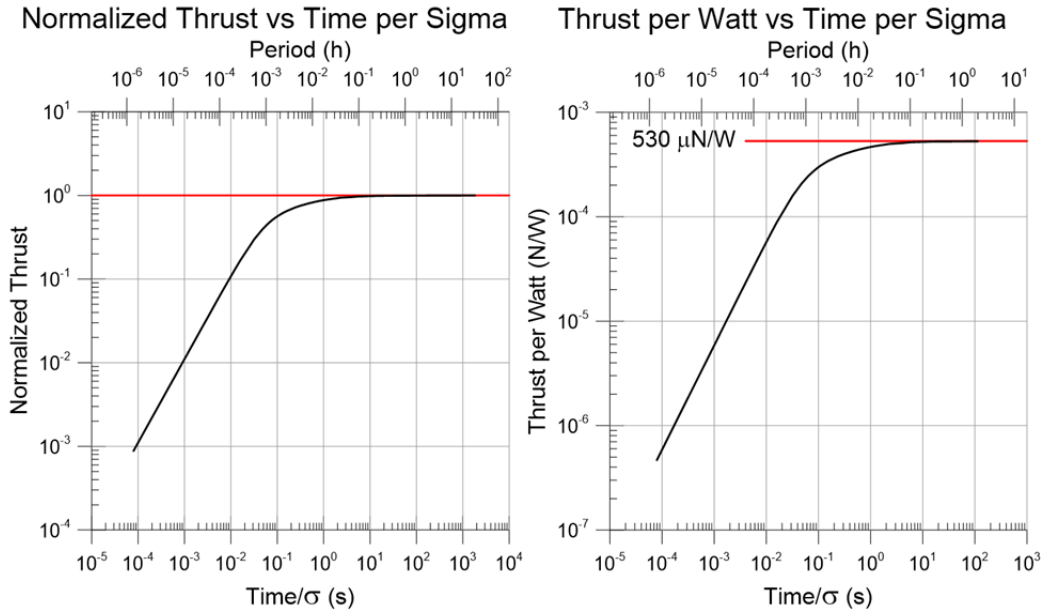
Figure 5. and 6. Thrust per Watt and normalized thrust relative to maximum thrust vs time per sigma for the case of a 1 m diameter SiO$_2$ asteroid, a laser power of 1 MW and a σ of 50 mm. This is a DE-STARLITE mission.

The model uses a directed energy beam, striking the surface of an asteroid. It is assumed that all the laser power is in the central spot (encircled energy), while in practice this will vary depending on the optical design with typical values being about 50-80%. The asteroid is represented with a rotating sphere composed of SiO$_2$. Given a σ of 50 mm, a laser power of 1 MW, and a 1 m diameter asteroid, rotation period of the asteroid was varied. The flux on the target is approximately 6.4×10^7 W/m^2, which, as stated earlier, is sufficient to induce efficient mass ejection.
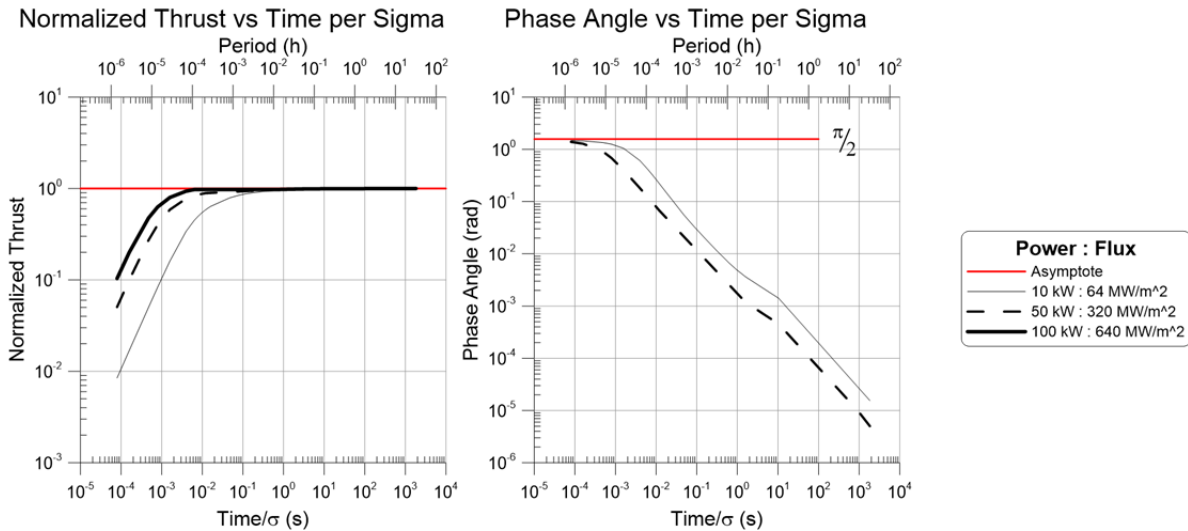
Figure 7. Normalized thrust relative to maximum thrust and phase angle vs period and time per sigma for the case of an SiO$_2$ 0.1 diameter asteroid and a σ of 5 mm. This is a DE-STARLITE mission.

The 10, 50, and 100 kW cases all increase rapidly until about 1 second. Notice that the thrust is extremely sensitive to temperature. Given various asteroid compositions, laser powers, and fluxes, figure 8 shows the general trends that the maximum and minimum temperatures follow. Figure 10 shows the normalized thrust for the same cases as fig. 8. From these figures, the conclusion can be drawn that temperature, asteroid, composition, and flux are all significant factors in computing the net thrust.
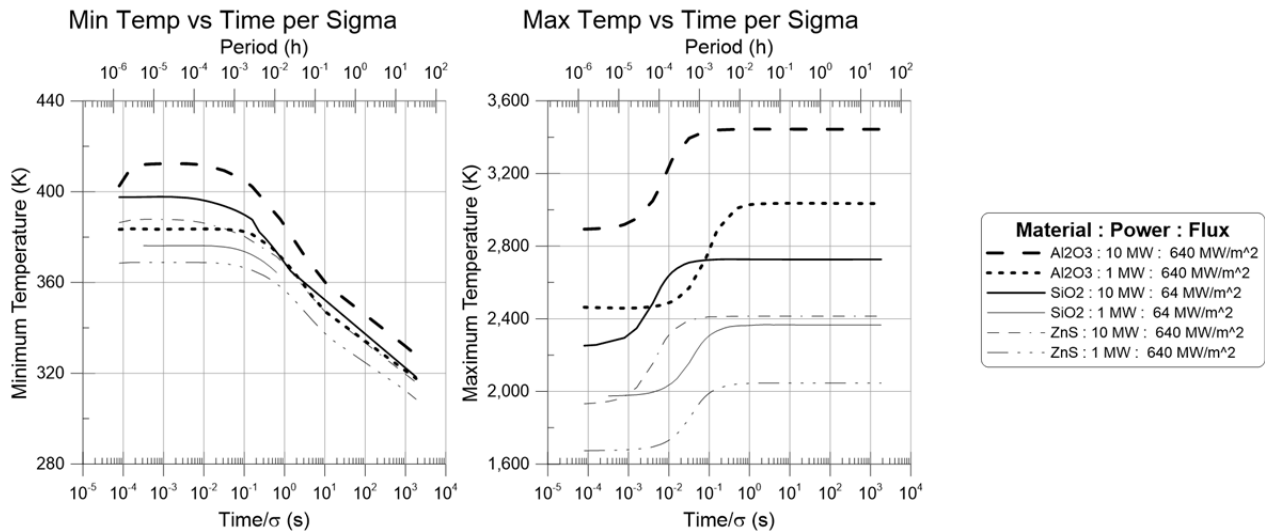
Figure 8. Minimun and maximum temperature vs period and time per sigma for a 1 m diameter asteroid and a σ of 50 mm. Assuming the average solar flux to be 350 W/m².

Calculations are performed in the reference frame of the asteroid. The coordinate system is defined such that the laser beam lies on the x-axis and points in the –x direction and the asteroid rotates counterclockwise (from x to y) about the z-axis. In Fig. 9, as the rotation period increases, the x-component of thrust increases and becomes relatively close to the thrust magnitude, while the thrust components in the y and z both approach 0. The y component decreases at short time per sigma, as there is insufficient time to generate strong mass ejection, while at large times the y component is small due to cooling. There is a maximum y component thrust around a few seconds per sigma. The z component is always small, since the asteroid rotates in the x-y plane.
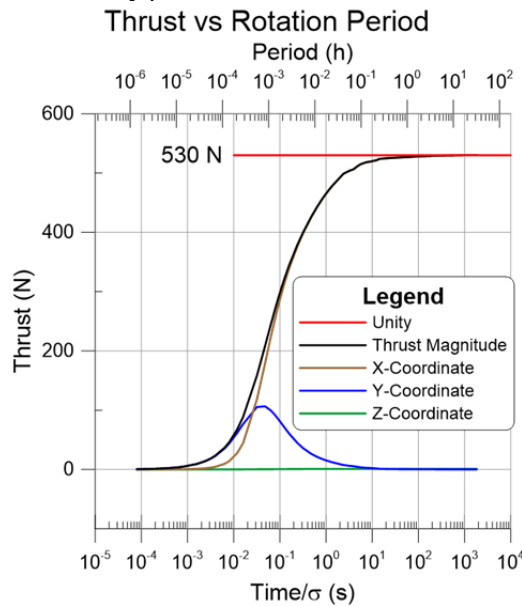

Figure 9. This figure shares the same parameters as Figures 5 and 6 (laser power of 1 MW, σ of 50 mm, 1 m diameter). It plots the x, y, and z components and magnitude of the normalized thrust as well as the overall thrust against the rotation period.

As an asteroid rotates, the laser spot ablates a portion of the asteroid, which revolves away from the spot and begins cooling. While it cools, high surface temperatures and flux levels indicate that this portion of the asteroid is still

being ablated. Thus, the surface continues to induce a vapor pressure and a thrust even when it is not beneath the laser spot. This then adds a component to the thrust vector that is not in the direction of the laser. This can be observed in Fig. 9, where the y-component of thrust is nonzero.

From rotational mechanics, as an asteroid's angular velocity increases, its rotation period decreases. Given that the y direction is perpendicular to both the laser direction (x) and the asteroid's axis of rotation (z), the phase angle is defined here to be the inverse sine of the y-component of thrust divided by the net thrust. With a decrease in rotation period, simulations show that the phase angle approaches a horizontal asymptote of $\pi/2$ radians.
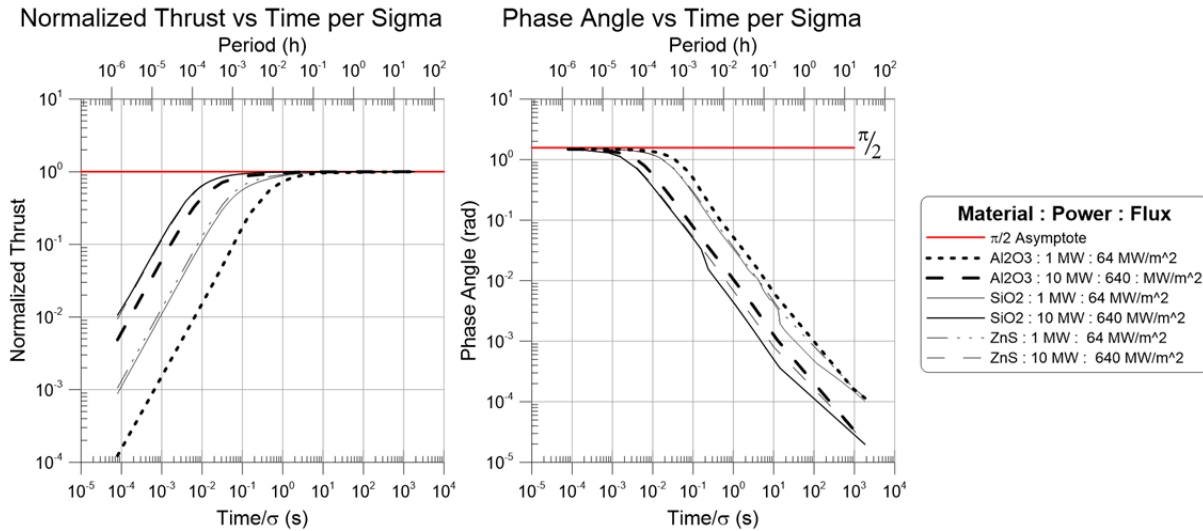
Figure 10. Calculated normalized thrust relative to maximum thrust and phase angle vs. rotation period for multiple compounds with various parameters. These are the same cases that are seen in figure 8: 1 m diameter asteroid and a σ of 50 mm, assuming the average solar flux to be 350 W/m².

This result means that greater asteroid angular velocities will increase the y-component of the thrust vector. This conclusion will have a significant impact on asteroid steering (direction and manipulation) at high angular velocities. As seen in Fig. 10, the trend is continuous, across various cases.

Figure 10 shows the normalized thrust vs time per sigma for the same various cases as Fig. 8 and 10. Observe that, as the minimum temperature increases, the normalized thrust also increases. Each case has many variables that must be taken into consideration. While the DE-STARLITE cases above used a 0.1 m diameter asteroid, figure 10 use a 1 m asteroid. These larger diameters cause the laser beam's energy to disperse across the surface of the asteroid, leading to a less concentrated laser spot, lower maximum temperature, and, consequently, less thrust.
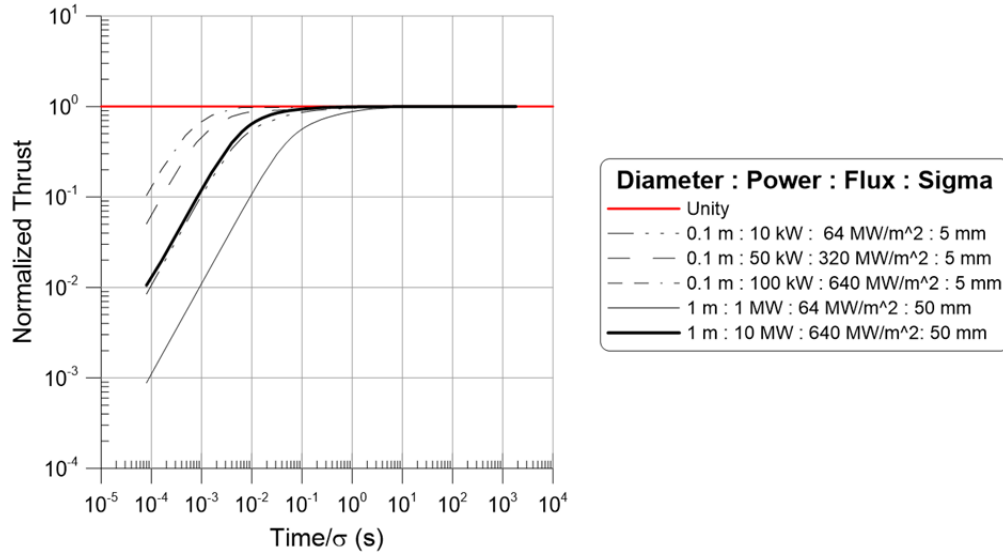
Normalized Thrust vs Time per Sigma

Figure 11. Calculated Normalized thrust relative to maximum thrust vs. rotation period for multiple compounds with various parameters. These are the same cases that are seen in figures 11.

5.   CHANGING THE SPIN RATE OF AN ASTEROID

5.1. De-spinning a Rotating Asteroid

The application of de-spinning asteroids is noteworthy for several reasons including: mining and ablation enhancement. The composition of asteroids is known to include many valuable elements and compounds, including water (a rare resource in space) as well as refinery-grade nickel and iron.[8] However, to mine these valuable resources, the asteroid must either be de-spun (so a lander can mine) or spun up (so the asteroid breaks apart and its remains can be scavenged). Additionally, as mentioned above, when an asteroid rotates, the energy from the laser beam smears across the surface; this decreases efficiency and adds a thrust vector in an undesirable direction. De-spinning asteroids would achieve both goals. Additionally, NASA and JPL are interested in this technology for their upcoming ARM mission, where they plan to catch an asteroid after DE-STARLITE de-spins it.

With laser ablation technology, it is possible to alter the spin of an asteroid. The small spot and fine control allow precision manipulation of the target. According to Fig. 12, the time it takes to de-spin an asteroid depends on thrust (torque); however, other factors include initial angular velocity and asteroid diameter. Simple steps allow calculating the torque necessary to de-spin a rotating spherical solid, assuming homogeneous composition and density. There are three ways the torque can be varied: by changing the power level, altering the spot size, or by moving the spot to different locations relative to the spin axis. Assuming a homogeneous spherical asteroid, the analysis is straightforward.

Assuming that the force F is applied at the edge of the asteroid with lever arm $0 < s < R$, the torque (τ) is F times s. Thus, for a constant thrust, the torque and angular acceleration are both constant. To find the desired time to despin, the initial rotation speed ω_0, which is $\frac{2\pi}{T}$ where T is the initial rotation period in seconds. To despin an asteroid in time t, the final velocity should be zero: $\omega_{final} = \omega_0 - \alpha t = 0$. Solved for acceleration, this is $\alpha = \frac{\omega_0}{t}$. To find the force required to despin an asteroid, the following steps can easily be performed. Fig. 12 shows the plotted result of these calculations. Note that the force scales as the fourth power of the radius and inversely as the rotation period (T) and desired spin down time (t).

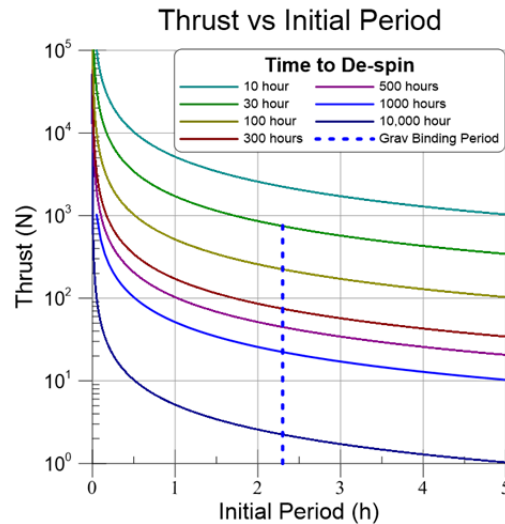$$\text{The mass of a sphere is } M = \rho \times \frac{4}{3}\pi R^3 \tag{5.1.1}$$

The momenet of inertia for a sphere is $I = \frac{2}{5}MR^2 = \frac{2}{5}\left(\rho \times \frac{4}{3}\pi R^3\right)R^2 = \rho\frac{8\pi R^5}{15}$.   (5.1.2)

Thus, the required torque is $\tau = I\alpha = \left(\rho\frac{8\pi R^5}{15}\right) \times \left(\frac{2\pi}{t \times T}\right) = \frac{\rho \times \frac{16}{15}\pi^2 R^5}{t \times T}$ (5.1.3)

and the required thrust is $F = \frac{\tau}{s} = \left(\frac{8\pi}{15}\rho R^5 \frac{\omega_0}{t}\right)\left(\frac{1}{s}\right) = \frac{\rho \times \frac{16}{15}\pi^2 R^5}{s \times t \times T}$.   (5.1.4)

Assuming s=R, then $F = \frac{\rho \times \frac{16}{15}\pi^2 R^4}{t \times T}$.   (5.1.5)

Figure 12. Thrust required as a function of rotation period (hours) to de-spin a 150 m diameter asteroid with a density of 2 000 kg/m^3.

5.2. Laboratory Results of De-Spinning Asteroids

An extremely low friction setup was developed with realistic rotation and a low-pressure environment to simulate a space environment. The speed of rotation was measured using a laser tracking system that reflected a secondary laser off of two mirrors, that were mounted on either side of the spindle, and then swept across a laser centroid detector, which then measured the rotation rate. This resulted in the laser ablation being capable of quickly de-spinning the asteroid and even reversing the direction of rotation. A future paper will present the detailed experimental, which roughly agree with the results stated above.

A video of a spinning target being de-spun is available on our website: www.deepspace.ucsb.edu/projects/directed-energy-planetary-defense.

6.   CONCLUSIONS

Directed energy is a feasible mechanism for diverting the trajectories of asteroids that threaten to impact Earth. With sufficient flux, surface material on the asteroid will evaporate, creating a reactionary force as the ejected material leaves the asteroid. Asteroids commonly rotate with respect to their orbital frames, and rotation will affect the manner in which a directed energy beam deflects the asteroid. A multi-physics model of a rotating asteroid has been formulated,

based on physical principles of the thrust generated by evaporation of surface material. Many simulations have been performed to characterize the effects of rotation on thrust. Reasonable rotation rates will have only modest effects on deflection, while very rapid rotators will have a large effect on deflection potential. It is also possible to de-spin an asteroid, thus increasing the potential to deflect its orbit and provide valuable aid for future capture or asteroid mining efforts.

ACKNOWLEDGMENTS

REFERENCES

[1] Lubin, P., Hughes, G.B., Bible, J., Bublitz, J., Arriola, J., Motta, C., Suen, J., Johansson, I.E., Riley, J., Sarvian, N., Clayton-Warwick, D., Wu, J., Milich, A., Oleson, M., Pryor, M., Krogen, P., Kangas, M., and O'Neill, H. "Toward Directed Energy Planetary Defense," *Optical Engineering*, Vol. 53, No. 2, pp 025103-1 to 025103-18 (Feb 2014), doi: 10.1117/1.OE.53.2.025103.

[2] Isabella E. Johansson[a], Tatiana Tsareva[b], Janelle Griswold[b], Philip Lubin[c], Gary B. Hughes[d], Hugh O'Neill[e], Peter Meinhold[c], JonathanSuen[c], QichengZhang[c], Jordan Riley[c], Carl Melis[f], Kevin Walsh[g], Travis Brashears[c], Justin Bollag[c], Shana Mathew[c] and Johanna Bible[c]. "Effects of asteroid rotation on directed energy deflection," *Proc. SPIE* 9226, Nanophotonics and Macrophotonics for Space Environments VIII, 92607 (September 17, 2014) doi:10..1117/12.2061368

[3] Mueller, M., "Surface Properties of Asteroids from Mid-Infrared Observations and Thermophysical Modeling," (2007).

[4] Mueller, Michael, Alan W. Harris, and Alan Fitzsimmons. "Size, albedo, and taxonomic type of potential spacecraft target Asteroid (10302) 1989 ML." *Icarus* 187.2 (2007): 611-615.

[5] Harris, A. W., "A Thermal Model for Near-Earth Asteroids," *Icarus* 131, 291-301 (1998).

[6] Delbò, M., Cellino, A., Tedesco, E. F., "Albedo and Size Determination of Potentially Hazardous Asteroids: (99942) Apophis," Icarus 188, 266-270 (2007).

[7] Margot, J. L., Nolan, M. C., Benner, L. A. M., Ostro, S. J., Jurgens, R. F., Giorgini, J. D., ... & Campbell, D. B. (2002). Binary asteroids in the near-Earth object population. *Science*, 296(5572), 1445-1448(2002).

[8] [http://www.planetaryresources.com/asteroids/composition/]

[9] Riley, J., Lubin, P., Hughes, G.B., O'Neill, H., Meinhold, P., Suen, J., Bible, J., Johansson, I., Griswold, J. and Cook, B. "Directed energy active illumination for near-Earth object detection," Conditionally Accepted for publication by *Journal of Astronomical Telescopes, Instruments and Systems* (Oct, 2014).

[10] Kosmo, K., Pryor, M., Lubin, P., Hughes, G.B., O'Neill, H., Meinhold, P., Suen, J., Riley, J., Griswold, J., Cook, B.V., Johansson, I.E., Zhang, Q., Walsh, K.J., Melis, C., Kangas, M., Bible, J., Motta, C., Brashears, T., Mathew, S. and Bollag, J. "DE-STARLITE - a practical planetary defense mission," *Nanophotonics and Macrophotonics for Space Environments VIII*, edited by Edward W. Taylor, David A. Cardimona, Proc. of SPIE Vol. 9226, pp. 922604 (Aug, 2014).

[11] Bottke Jr, William F et al. "The Yarkovsky and YORP effects: Implications for asteroid dynamics." *Annu. Rev. Earth Planet. Sci.* 34 (2006): 157-191.